Available online at www.sciencedirect.com

ScienceDirect

Energy Procedia 102 (2016) 144 – 151

Energy Procedia

E-MRS Spring Meeting 2016 Symposium T - Advanced materials and characterization techniques for solar cells III, 2-6 May 2016, Lille, France

Photosensitive defects in Gd_2O_3 – advanced material for solar energy conversion

Anatoly Zatsepin, Yulia Kuznetsova, Luisa Spallino*, Vladimir Pustovarov, Vladimir Rychkov

Ural Federal University, 19 Mira Street, 620002 Ekaterinburg, Russia

Abstract

The photo- and thermally- stimulated luminescence of Gd_2O_3 and Gd_2O_3:Zn nanostructured powders has been investigated at 295 and 90 K. Optically active impurities and intrinsic defects in the host lattice have been detected. The kinetics parameters of the charge trapping centers (order of kinetics, activation energy, frequency factor) were determined. The nature of defect states and their role in the processes of the energy relaxation are discussed.

© 2016 The Authors. Published by Elsevier Ltd. This is an open access article under the CC BY-NC-ND license (http://creativecommons.org/licenses/by-nc-nd/4.0/).

Peer-review under responsibility of The European Materials Research Society (E-MRS).

Keywords: gadolinium oxide; photoluminescence; thermoluminescence; intrinsic defects; solar energy

1. Introduction

The phosphors based on lanthanides represent a perspective class of materials for photovoltaic devices. One of the main features of rare earth (RE) ions is a large number of discrete energy levels that form the 4*f* electronic shell [1]. The variety of optical transitions in a wide spectral range has the potential to be used for down- and up-conversion processes. These energy transfer mechanisms are the basis for the functioning of the so-called luminescent solar concentrators that are placed on the front or rear side of traditional Si solar cell as additional layers. Such structures allow one to use the additional fraction of solar spectrum in UV and NIR region, therefore, enhancing the conversion efficiency [2, 3].

Among the compounds containing the RE elements, the gadolinium oxide (Gd_2O_3) is a good candidate as host

* Corresponding author.
E-mail address: lspallino@urfu.ru

1876-6102 © 2016 The Authors. Published by Elsevier Ltd. This is an open access article under the CC BY-NC-ND license (http://creativecommons.org/licenses/by-nc-nd/4.0/).
Peer-review under responsibility of The European Materials Research Society (E-MRS).
doi:10.1016/j.egypro.2016.11.329

matrix of luminescence layers. In fact, it has remarkable optical and chemical properties, such as the transparency in the visible spectral region (E_g = 5.6 eV), low energy of phonons (≈ 600 cm^{-1}), high refractive index, good chemical durability and thermal stability [4, 5]. In addition, the similarity between the Gd^{3+} and RE^{3+} ionic radii and the electronic shell structures provide the possibility to create different pairs of rare earth ions (for example, Yb-Er, Yb-Ho, Yb-Tm) [6]. All these features make Gd_2O_3 a promising material for down- and up-conversion applications in solar energy.

The enhancement of the Si solar cells efficiency by means of the luminescence solar concentrators is directly determined by energy transfer mechanisms of the donor-acceptor couples in the optically active layers. Matrix imperfections are one of the main responsible for the energy migration processes. In general, one supposes that the structural defects in the host lattice lead to the decrease of the overall luminescence efficiency due to the creation of non-radiative relaxation channels [7]. However, there is information about improving the luminescence efficiency of RE-doped phosphors containing the structural distortions [8]. Thus, the investigation of the effect induced on the spectral-optical properties of RE-doped materials by intrinsic host lattice defects could be of great interest for improving the functional characteristics.

2. Samples and methods

The microstructured nominally pure Gd_2O_3 powder was prepared at Ural Federal University. Gadolinium nitrate ($Gd(NO_3)_3$) with a purity of at least 99.99 % was used as precursor and was dissolved in a mixture of water and isopropyl alcohol at concentration of 50 g/l. The suspension was firstly kept under stirring for 30 minutes and then was filtrated, dried and calcinated at 1000° C for 2 hours. The Gd_2O_3:Zn compacted powder was synthesized by sol-gel method at the Institute of Physics Polish Academy of Sciences. The gadolinium (Gd_2O_3) and zinc (ZnO) oxides as starting materials were kept in 1M HCl solution for 24 h, the molar concentration being 80 and 20 % respectively. The solution was firstly centrifuged for 15 min at 22° C and the deposited material, separated by supernatant, was repeatedly washed with a mixture of water and ethanol by centrifuging at the same conditions. The obtained gel powder was dried in air and annealed at 1000° C for 2 hours.

The XRD profile of Gd_2O_3 sample showed single cubic phase (Ia-3 space group) with lattice constant a = 10.81 Å The Gd_2O_3:Zn sample has a monoclinic crystal phase (space group C2/m) with lattice parameters a = 14.09 Å, b = 3,57 Å and c = 8,76 Å. The average particle sizes of both powders were estimated to be 10-40 nm by using the Debye-Scherrer's method [9].

The photoluminescence (PL) and PL excitation studies were performed using a 400 W deuterium lamp, a R6358-10 Hamamatsu photomultiplier and two prismatic DMR-4 monochromators with the spectral resolution of 1 nm in the visible spectral region. Low-temperature measurements were carried out in a cryostat at $P = 10^{-4}$ Pa. The temperature of the sample was controlled by a platinum resistance thermometer HRTS-5760-B-T-1-12. The thermally stimulated luminescence (TL) spectra were recorded in the spectrally integrated mode in the region 300-600 nm at a constant heating rate of 0.3 K/s. The samples were previously subjected to X-ray irradiation with exposure dose of 50 kR at room temperature.

3. Results

In Fig. 1(a) the PL spectrum emitted by Gd_2O_3 sample is reported. It is acquired at ambient temperature under interband excitation at 5.4 eV. It evidences strong and sharp lines at 2.4, 2.6 and 2.8 eV and a weaker band at 4.1 eV. The observed emission in the visible region is characteristic of 4*f*-4*f* intraconfiguration optical transitions in europium (Eu^{3+}), terbium (Tb^{3+}) and praseodymium (Pr^{3+}) ions. One can assume that these ions are in the Gd_2O_3 matrix as micro impurities. The band observed at 4.1 eV can be attributed to the ${}^6P_J \rightarrow {}^8S_{7/2}$ optical transition in Gd^{3+} ion. Generally, the luminescence of host ions is not typical and can indicate the structure distortions in lattice. In order to obtain detailed information about the emission centers and luminescence mechanisms we performed low-temperature measurements.

As can be seen from Fig. 1(b) broad non-elementary band is observed under the excitation of 5.4 eV at 90 K. As shown by the black dotted lines it can be decomposed into two Gaussian components with maximums at 2.7 eV (FWHM ≈ 0.8 eV) and 3.3 eV (FWHM ≈ 0.9 eV).

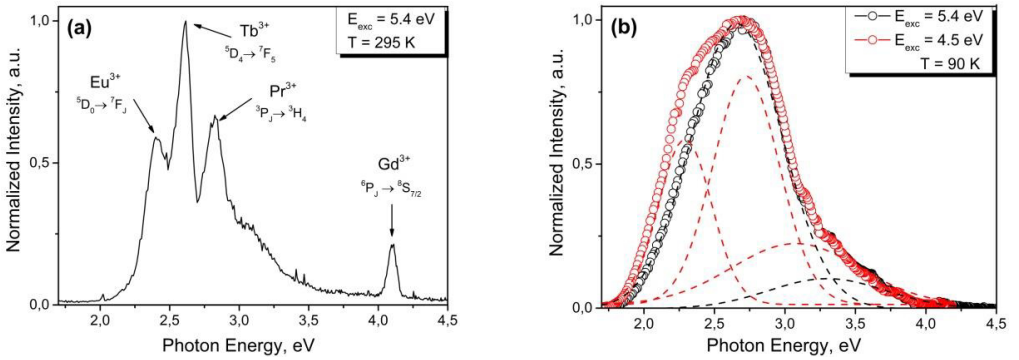

Fig. 1 – PL spectra of Gd_2O_3 at temperatures of 295 K (a) and 90 K (b) and 5.4 and 4.5 eV excitations.

Since the emission of both RE impurity ions and host Gd^{3+} ions are not detected at low temperature, we have tried to implement the selective excitation at 4.5 eV that corresponds to the ${}^6I_J$ high-energy state of Gd^{3+}. It resulted in the qualitative change in PL spectrum. Along with the bands registered in the case of interband excitation, the new band with maximum at 2.3 eV and FWHM ≈ 0.4 eV has been detected by the Gaussian decomposition. The observed differences in comparison with the PL spectrum recorded at room temperature indicate that, on decreasing the temperature, other optical centers are active. Moreover, these centers act as killers of RE ions luminescence.

The excitation spectrum of RE luminescence recorded at 295 K (blue, red and green lines) and that of the low-temperature band of 2.7 eV (black line) are shown in Fig. 2. It can be seen that the excitation corresponding to interband transitions of the Gd_2O_3 host lattice is the most effective. In addition, the group of bands at 4, 4.5 and 4.8 eV associated with ${}^6P_J$, ${}^6I_J$ and ${}^6D_J$ excited states of Gd^{3+} ion have been registered [10].

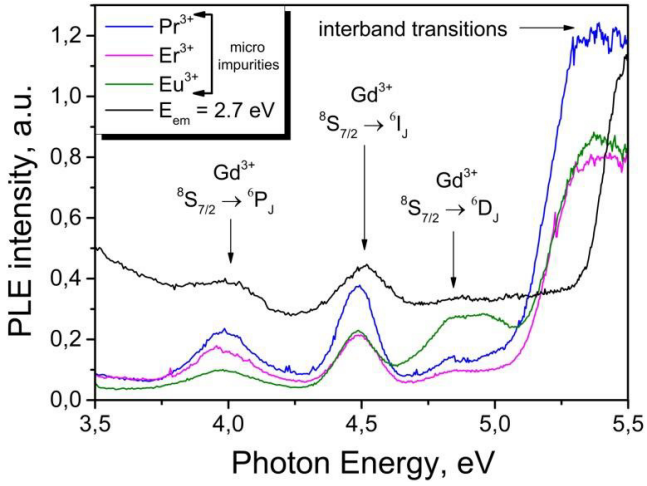

Fig. 2 – The excitation spectra of RE impurity ions luminescence and low-temperature 2.7 eV emission in Gd_2O_3.

This fact, along with the absence of any bands corresponding to intracenter absorption of Pr^{3+}, Er^{3+} and Eu^{3+} ions as well as the proximity of the positions of their energy levels with the excited levels of Gd^{3+} ions, indicates that the energy transfer from matrix Gd^{3+} ions to impurity RE centers takes place. Furthermore, the similarity of excitation spectra recorded for the band at 2.7 eV points out that Gd^{3+} ions also act as donors of energy to the optical centers which are responsible for the low-temperature luminescence.

The PL investigations allowed one to reveal optically active intrinsic defects in nanostructured Gd_2O_3 powder, however, the obtained data are not enough to establish the nature of these defect states, especially related to the low-temperature luminescence. Since our hypothesis is that the energy levels induced in forbidden gap by the lattice distortions serve not only as luminescence centers but also as trapping centers, we have performed the TL measurements. To induce free charge carriers in conduction and valence bands, the Gd_2O_3 sample was subjected to X-ray irradiation. The dependence of the luminescence intensity on the temperature recorded in the range of 300-475 K is shown in Fig. 3 by black triangles. Three maxima are observed at 344, 382 and 438 K. This finding indicates the creation of three types of traps.

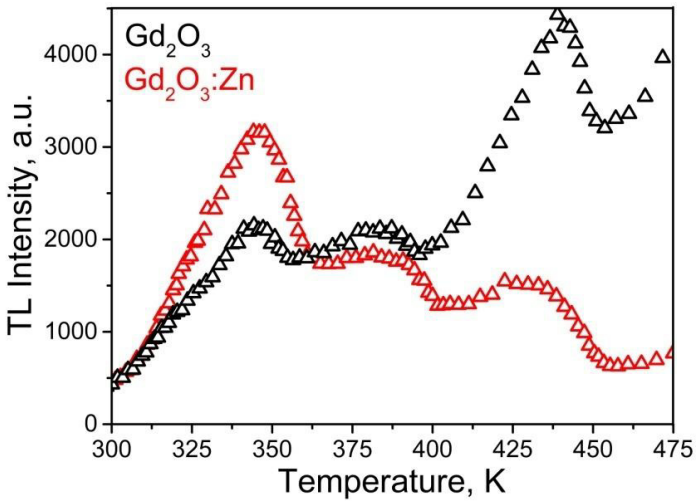

Fig. 3 –TL curves of Gd_2O_3 and Gd_2O_3:Zn samples after the X-ray irradiation at room temperature.

It is known that in oxides the positive charged oxygen vacancies are the most common type of trapping centers [11-13]. In order to confirm or refute the hypothesis that traps in Gd_2O_3 are related to the defects of anionic sublattice we have studied also the TL of Gd_2O_3: Zn sample (red triangles in Fig. 3). It has been supposed that Zn^{2+} ions involved in Gd_2O_3 lattice would lead to violation of stoichiometry and to creation of oxygen-related defects. By comparing the two TL spectra, there are no qualitative changes in the structure of TL glow curve of Gd_2O_3: Zn and Gd_2O_3. However, the redistribution between intensities of maximums corresponding to highest and lowest temperatures is observed. So, intensity of 344 K peak increases approximately 1.5 times, while the intensity of maximum at 438 K decreases nearly 3 times. This fact indicates that the concentrations of various types of traps are changed after the introduction of Zn^{2+} ions.

In order to give quantitative estimation of trapping parameters we used the Chen's empirical equation [14]:

$$E = \frac{2.52kT_m^2}{\omega} - 2kT_m\,, \tag{1}$$

where E is the activation energy characterizing the depth of trap; k is the Boltzmann constant; T_m is the peak temperature at the maximum TL intensity and ω is the full width at half maximum determined as difference between values of temperatures on either side of T_m that correspond to the half-maximum intensity. The form factor (so-called geometry or symmetry factor) μ_g is given as:

$$\mu_g = \frac{T_2 - T_m}{\omega}\,, \tag{2}$$

where T_2 is the temperature corresponding to half-maximum intensity by the side of peak's decay. It is accepted that the value of μ_g is close to 0.42 for first order kinetics and 0.52 for second order kinetics. The frequency factor S can be calculated by using the values of activation energy E, order kinetics b and heating rate β from the equation:

$$\frac{\beta E}{kT_m^2} = S\exp\left\{\frac{-E}{kT_m^2}\right\}\left[1+(b-1)\frac{2kT_m}{E}\right]. \quad (3)$$

The trapping parameters calculated for all revealed peaks in TL curves of Gd_2O_3 and Gd_2O_3: Zn samples are listed in Table 1.

Table 1. Parameters of trapping centers in Gd_2O_3 and Gd_2O_3: Zn samples.

T_m, K	Order of kinetics	Activation energy E, eV	Frequency factor S, s^{-1}
344	1	0.74	9.8×10^7
382	1	0.82	5.2×10^6
438	1	0.93	2.1×10^7

4. Discussion

As experimental results demonstrated, in spite of the Gd_2O_3 sample was implied as nominally pure, it has been found that it contains a certain percentage of impurities, in particular, the Eu^{3+}, Tb^{3+} and Pr^{3+} ions have been revealed by the PL study at 295 K (Fig. 1(a)). Such situation is not surprising since RE even in very low concentrations (a few thousandths of a percent) are characterized by relatively high radiation intensity and can significantly influence the spectral composition of the luminescence of the material under investigation.

The emission features of Gd_2O_3 are significantly changed on decreasing the temperature. The broad emission bands revealed at low temperature (Fig. 1(b)) can't be attributed to optical transitions in the trivalent RE ions as they are characterized by the line structure of the luminescence spectra. At the same time the oxidation degree of some RE (for example, Ce and Eu) may be equal not only +3 but also +2. The luminescence of divalent RE is due to the $5d\rightarrow4f$ optical transitions. Since $5d$ electronic shell is subjected to the strong influence of internal crystal field the broad emission bands are typical for RE in divalent state [15, 16]. However, their spectral positions are not correlated with the bands obtained in our spectra. The nature of the low-temperature intrinsic luminescence in Gd_2O_3 can be most likely related to the presence of anionic defects like F-centers. In literature [17] the broad band emission of Gd_2O_3 in the blue region of spectrum (≈ 3.4 eV) is assigned to the recombination of delocalized electron near the conduction band with the F^+ - center. From this point of view, we can assume that the two emission bands observed at 2.7 and 3.3 eV are due to the oxygen-deficient centers with different charge states.

The PL excitation spectra recorded at both 295 and 90 K indicate that one of the excitation channel of intrinsic emission in Gd_2O_3 is the energy transfer from host Gd^{3+} ions to the optically active centers (Fig. 2). It is likely that these ions can't be located in regular positions of Gd_2O_3 lattice and represent the local defects of cationic sublattice. The formation of such defective states may be caused by various reasons. One of the possible mechanisms is the thermal lattice disordering which leads to emergence of interstitial Gd^{3+} ions. Another reason could be the association of regular lattice cations with nearest point defects. In all cases the appearance of Gd^{3+} energy levels in the region of Gd_2O_3 transparency indicates that electron structure of cationic states is distorted. It is also confirmed by the line at 4 eV which is attributed to the own Gd^{3+} emission (Fig. 1(a)). Its weak intensity in comparison with the luminescence of the RE impurity ions is resulted from the low probability of the radiative optical ${}^6P_J\rightarrow{}^8S_{7/2}$ transition in Gd^{3+} due to the high efficiency of energy transfer from the excited states of the Gd^{3+} ion to the RE impurity centers. The schematic representation of Tb^{3+}, Eu^{3+} and Gd^{3+} energy levels as well as the most probable energy transfer pathways followed by radiative and non-radiative relaxations is shown in Fig. 4.

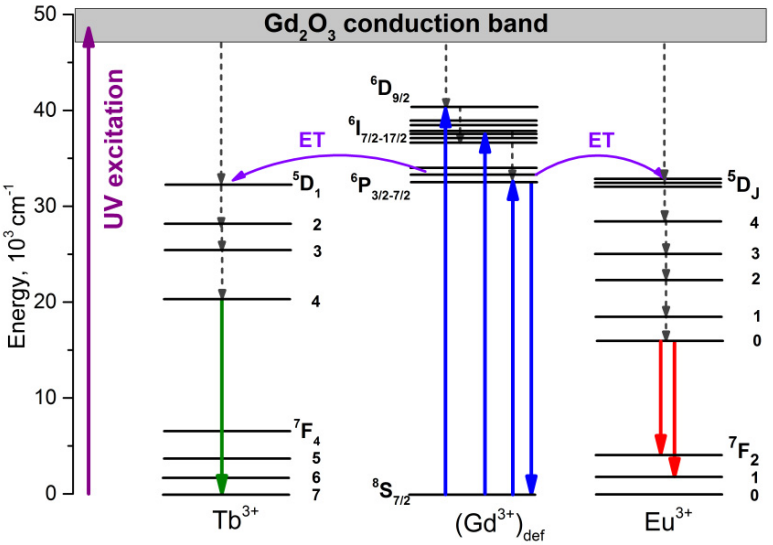

Fig.4 – The energy levels diagram of Tb^{3+}, Eu^{3+} optical centers and defective $(Gd^{3+})_{def}$ ions in Gd_2O_3 matrix. The energy transfer processes are shown by curved purple lines. Non-radiative relaxation and emission in visible spectral region are marked by black dotted and colored solid lines respectively.

The low-temperature luminescence is the most efficiently excited in the regions of fundamental absorption edge and formation of separated electron-hole pairs (Fig. 2). Electrons in conduction band can be trapped by the F^+ and F^{2+} - centers with the formation of excited $(F)^*$ and $(F^+)^*$ - centers respectively followed by their radiative relaxation:

$$F^+ + e \rightarrow (F)^* \rightarrow F + h\nu, \tag{4}$$

$$F^{2+} + e \rightarrow (F^+)^* \rightarrow F^+ + h\nu. \tag{5}$$

Moreover, it has been observed that the energy transfer from Gd^{3+} ions represents another channel of excitation of the vacancy type luminescent-active defects (Fig. 2). Excitation corresponding to the $^8S_{7/2} \rightarrow {}^6I_J$ optical transition in Gd^{3+} results in the appearance of new emission band at 2.3 eV (Fig. 1(b)). This band is most likely related to the radiative relaxation of another type of anionic defects – F^{2+} - centres. Due to the energy transfer from gadolinium ions, the F^{2+} - center can directly pass to the excited state with the subsequent radiative transition to the ground state. The excitation of the F and F^+ - centers can be realized by the analogous way that is confirmed by the 2.7 and 3.3 eV emission bands under the excitation of the Gd^{3+} high-energy state.

The obtained results evidence various types of intrinsic defects in Gd_2O_3 matrix. Several channels of excitation energy relaxation in defective Gd^{3+} ions have been revealed: (*i*) radiative transition $^6P_J \rightarrow {}^8S_{7/2}$; (*ii*) energy transfer to impurity RE centers; (*iii*) energy transfer to differently charged F – centers.

In order to obtain more complete information about the nature of anion-defective centers we have performed the measurements of thermally stimulated luminescence. The presence of three peaks in TL spectra of Gd_2O_3 indicate that X-ray irradiation creates three types of trapping centers with energy levels located at different depths from the bottom of conduction band (Fig. 3). Similar situation has been reported in [18] and the shallow and deep traps have been attributed to the oxygen-deficient centers. For more information about the nature of traps in Gd_2O_3 we also have studied the TL of Gd_2O_3:Zn sample. The ionic radii of Gd^{3+} (0.94 Å) and Zn^{2+} (0.83 Å) are close so it is more likely the Zn^{2+} ions occupy the cationic positions in Gd_2O_3 lattice by replacing the Gd^{3+} ions. For local charge compensation such substitution has to entail the creation of intrinsic defects in anionic sublattice. The mechanism of

charge compensation can be represented by following scheme:

$$Gd_2O_3 + 2Zn \rightarrow 2Zn_{Gd}^{'} + V_O^{\bullet\bullet} + 3O_O^{\times}, \quad (6)$$

where in accordance with Kroger-Vink symbols the $Zn_{Gd}^{'}$ stands for the Zn^{2+} ion which substitute the lattice site of Gd^{3+} with the formation of effective charge equal to -1; $V_O^{\bullet\bullet}$ represents the double charged oxygen vacancy and represents the oxygen at regular lattice position. Two acts of Gd^{3+} replacement by Zn^{2+} provide the formation of single oxygen vacancy with effective charge of +2. So the TL signal in Gd_2O_3:Zn is more probably related to the oxygen-deficient centers. Since the TL peaks positions remain unchanged after the introduction of Zn^{2+} ions in Gd_2O_3 lattice (Fig. 3) it can be a confirmation of the anion-defective nature of trapping centers in undoped sample. Thus we suppose that two maximums in TL curves are related to the ionization of *F*- and F^+- centers that correspond to the oxygen vacancies with two and one trapped electrons respectively and one more TL peak is likely due to the ionization of *F*-type aggregate.

In accordance with the scheme (eq. 6) the concentration of *F*-centres increases after the Zn^{2+} doping. The free charge carriers generated by the thermal ionization of F^+ - centers migrate through the conduction band and can be trapped by the deeper *F*-centers. Since the introduction of Zn^{2+} ions increases the number of anion-defective states of this type, it can be expected that the probability of electron localization at the level of the *F*-center will also increase. At the same time the destruction of *F*-centers is accompanied by the formation of F^+ - centers. On the basis of experimental data which demonstrate increasing the intensity of 344 K peak and decreasing maximum at 438 K we can suppose that the former peak is related to the F^+ - centers while the latter – to the *F*-centers.

Robertson et al. [19] have shown the results of calculation the position of oxygen vacancies energy levels in La_2O_3. It has been established that the level of F^{2+}-center is the nearest to the bottom of the conduction band while the state of neutral oxygen vacancy is the most remote and the level of F^+-center is localized between them. Taking into account the similarity of structure and properties of La_2O_3 and Gd_2O_3 one can suggest that the energy levels of anionic defects in Gd_2O_3 are located in the same order. In this case it's additional evidence that the high-temperature TL peak can be assigned to the ionization of *F*-center and low-temperature – to the ionization of F^+ - center. The nature of intermediate TL maximum at 382 K remains unclear at this stage of investigation. It can be supposed that there are aggregate centers of *F*-type or hole traps that are responsible for this peak.

5. Conclusion

The various types of intrinsic defects in Gd_2O_3 matrix have been revealed by investigation of photo- and thermally stimulated luminescence. It has been found that the Gd^{3+} ions occupying the irregular lattice positions act as donors of excitation energy to optically active anion-defective centers that are responsible for low-temperature emission. The luminescence bands at 2.3, 2.7 and 3.3 eV at this stage are attributed to the radiative relaxation of oxygen-deficient centers with different charge states (F^{2+}, F^+ and *F*- centres). It has been established that irradiation of samples by X-ray leads to the formation of traps corresponding to the 0.74, 0.82 and 0.93 eV activation energies and deeper and shallower centers are most likely related to the F^+- and *F*- centers. Violation of oxygen stoichiometry by Zn^{2+} induces the redistribution of traps concentrations due to the increasing of *F*-states. The findings can be used for prediction of properties of down- and up-conversion materials based on lanthanides and also to act on the functional parameters of energy conversion devices.

Acknowledgements

This work was supported by the Ministry of Education and Science of Russia, the Grain-in-Aid Agreement no. 14.581.21.0002, September 29, 2014 (the unique identifier RFMEFI58114X0002) in the frame of the Federal Aim Program «Research and Development in Priority Directions of the Science and Technology Complex of Russia for 2014-2020». The part of results was obtained within the framework of the Act 211 of Government of the Russian Federation, contract № 02.A03.21.0006 and carried out in the framework of state assignment of Russian Federation Ministry of Science and Education (3.1016.2014/K). The author L. Spallino acknowledges for the financial support of the RFBR (Russian Foundation for Basic Research) 2016/2018 (Project N° 16-32-60063).

References

[1] Correia FH, Bermudez VZ, Ribeiro JL, Andr´e PS, Ferreira AS, Carlos DL. Luminescent solar concentrators: challenges for lanthanide-based organic–inorganic hybrid materials. *J. Mat. Chem. A* 2014;2:5580-96.
[2] Shalav A, Richards BS, Green MA. Luminescent layers for enhanced silicon solar cell performance: Up-conversion. *Sol. Energ. Mat. Sol. C.* 2007;91:829-42.
[3] Richards BS. Luminescent layers for enhanced silicon solar cell performance: Down-conversion. *Sol. Energ. Mat. Sol. C.* 2006;90:1189-1207.
[4] Guo H, Dong N, Yin M, Zhang W, Lou L, Xia S. Visible Upconversion in Rare Earth Ion-Doped Gd_2O_3 Nanocrystals. *J. Phys. Chem. B* 2004;108:19205-9.
[5] Singh SK, Kumar K, Rai SB. Multifunctional Er^{3+}–Yb^{3+} codoped Gd_2O_3 nanocrystalline phosphor synthesized through optimized combustion route. *Appl. Phys. B* 2009;94:165-73.
[6] Gai S, Yang P, Wang D, Li C, Niu N, Hea F, Lia X. Monodisperse Gd2O3:Ln (Ln: Eu3+, Tb3+, Dy3+, Sm3+, Yb3+/Er3+, Yb3+/Tm3+, and Yb3+/Ho3+) nanocrystals with tunable size and multicolor luminescent properties. *Cryst. Eng. Comm.* 2011;13:5480-87.
[7] Case MA, Bradford CS. *Photoluminescence: Applications, types and efficacy.* New York: Nova Science Publishers, Inc.;2012, p. 55.
[8] Liu B, Gu M, Liu X, Ni C, Wang D, Xiao L, Zhang R. Effect of Zn^{2+} and Li^{+} codoping ions on nanosized Gd_2O_3:Eu^{3+} phosphor. *J. Alloy. Compd.* 2006;440:341-5.
[9] Klug P and Alexander LE. *X-ray Diffraction Procedure*. New York: Wiley;1954.
[10] Wegh RT, Donker H, Meijerink A. Vacuum-ultraviolet spectroscopy and quantum cutting for Gd^{3+} in $LiYF_4$. *Phys. Rev. B* 1997;56:841-8.
[11] Rodrigues JA and Garcia MF. *Synthesis, Properties, and Applications of Oxide Nanomaterials.* New York: Wiley;2007.
[12] Ganduglia-Pirovano MV, Hofmann A, and Sauer J. Oxygen vacancies in transition metal and rare earth oxides: Current state of understanding and remaining challenges. *Surf. Sci. Rep.* 2007;62:219-70.
[13] Tanaka I, Oba F, Tatsumi K, Kunisu M, Nakano M, and Adachi H. Theoretical formation energy of oxygen vacancies in oxides. *Mater. Trans.* 2002;43:1426-29.
[14] Chen R, Kirish Y. *Analysis of Thermally Stimulated Processes*. New York: Pergamon;1981.
[15] Liu Z, Nengli D, Yang L, Li J. High-efficient near-infrared quantum cutting based on broadband absorption in Eu^{2+}–Yb^{3+} co-doped glass for photovoltaic applications. *Appl. Phys. A* 2015;119:553-7.
[16] Liu Z, Li J, Yang L, Chen Q, Chu Y, Dai N. Efficient near-infrared quantum cutting in Ce^{3+}–Yb^{3+} codoped glass for solar photovoltaic. *Sol. Energ. Mat. Sol. C.* 2014;122:46-50.
[17] Dhananjaya N, Nagabhushana H, Nagabhushana BM, Rudraswamy B, Sharma SC, Sunitha DV, Shivakumara C, Chakradhar RPS. Effect of different fuels on structural, thermo and photoluminescent properties of Gd_2O_3 nanoparticles. *Spectrochim. Acta A* 2012; 96**:** 532-40.
[18] Tamrakar RK, Bisen DP. Thermoluminescence studies of ultraviolet and gamma irradiated erbium(III)- and ytterbium(III)-doped gadolinium oxide phosphors. *Mat. Sci. Semicon. Proc.* 2015:33;169-88.
[19] Robertson J, Xiong K, Clark SJ. Band gaps and defect levels in functional oxides. *Thin Solid Films* 2006;496:1-7.